

Critical behavior of power transmission network complex dynamics in the OPA model

Cite as: Chaos 29, 033103 (2019); doi: 10.1063/1.5066370
Submitted: 15 October 2018 · Accepted: 7 February 2019 ·
Published Online: 1 March 2019



View Online



Export Citation



CrossMark

Benjamin A. Carreras,^{1,2}  José M. Reynolds-Barredo,¹  Ian Dobson,³  and David E. Newman²

AFFILIATIONS

¹Departamento de Física, Universidad Carlos III de Madrid, 28911 Leganes, Madrid, Spain

²Physics Department, University of Alaska, Fairbanks, Alaska 99775, USA

³Electrical and Computer Engineering Department, Iowa State University, Ames, Iowa 50011, USA

ABSTRACT

Many complex infrastructure systems, such as electric power transmission grids, display characteristics of a critical or near critical behavior with a risk of large cascading failures. Understanding this risk and its relation to the system state as it evolves could allow for a more realistic risk assessment and even for mitigation measures. We use the OPA model of cascading blackouts and grid evolution to describe and quantify regimes of criticality of the power grid.

Published under license by AIP Publishing. <https://doi.org/10.1063/1.5066370>

Complex systems can operate in critical or near critical conditions. While this regime may be efficient because less resources are required, it is also risky, because widespread cascading failures can occasionally occur that are costly to our society. One example is cascading blackouts in power grid transmission networks. Here, we analyze power grids using simplified networks with characteristics similar to that of real systems but computationally more accessible. We apply several measures of criticality to reveal different regimes of the complex dynamics as the reliability of transmission lines changes, including a critical regime showing power laws in the distribution of blackout size and sub- and super-critical regimes with lognormal distributions of blackout size. A simple model of the lognormal behavior away from criticality is also suggested.

I. INTRODUCTION

Complex critical infrastructure systems, such as power transmission grids, are prone to cascading failures of all sizes.^{1,2} This is a characteristic property of complex systems operating near their critical point.^{3–7} In estimating the risk of large blackouts, it is necessary to find out how close the system is to the critical point. In this paper, we explore this criticality issue using the ORNL-PSerc-Alaska (OPA) model.^{3,8,9} The OPA model of an electric power transmission system is based on the complex dynamics of the opposing forces of

increasing power demand and the engineering responses to failure. These complex dynamics drive the system to a self-organized critical state (SOC).¹⁰ The OPA model has been validated^{11,12} using North American power transmission data from the Western Electricity Coordinating Council (WECC).

The system's average proximity criticality depends on the properties of the system, such as the reliability of the power lines and the rate of upgrade of the system. In the OPA model, these properties are quantified through parameters that correspond to these overall properties, so that we can study the level of criticality of the system through systematic variations of the parameters. We explore the changes in the properties of the dynamical evolution of the electric power grid as we change the reliability of the lines, that is, the probability p_1 that an overloaded line outages during the cascading process. We study these changes as the system gets closer to a critical point using the 1600 node artificial network developed in Ref. 16. (Earlier studies were carried out using a smaller network,¹¹ but the network was likely too small to be able to detect clear changes when the system was getting close to a critical point.)

We evaluate the criticality by processing the cascades produced by the OPA model. The λ measure of average cascade propagation is the standard Harris estimator¹⁴ calculated by taking the average of the ratio of child failures (iteration i) to parent failures (iteration $i - 1$) over all the cascading events. In Ref. 13, we developed the λ_{gaga} measure to determine the criticality of the dynamic states during the electric

grid time evolution. The λ_{gaga} measure is an averaged value of the parameter λ measured during the cascading process of the blackout normalized to the maximum possible length of the cascades.

In a dynamical process, we have to distinguish between the overall dynamical state of the system and the individual states at each moment of the dynamical evolution. So for a fixed set of parameters, we also explore the critical properties of individual states depending on the instantaneous level of the demand. In reality, the averaged statistical properties of the dynamical states result from a mixture of states at different levels of criticality.

The rest of the paper is organized as follows. Section II describes the OPA model. Section III uses the OPA model to explore the criticality as a function of the reliability parameter of the lines. These results give us three different regions on this parameter and they are discussed in detail in Sec. IV. Section V tests the fits of the various blackout probability distribution functions (PDFs) with the power law and lognormal distributions using Clauset's method.¹⁷ Section VI uses a simple model to interpret the critical behavior. Then, we explore states within the same dynamical simulation with different levels of criticality. Finally, the conclusions of the paper are given in Sec. VIII.

II. THE OPA MODEL

The OPA model as described in Refs. 3, 8, and 9 has two time scales: a fast time scale of cascading blackouts and a slow time scale of grid evolution as summarized in Fig. 1. In the fast time scale, OPA simulates a process of cascading outages with transmission lines, loads, and generators represented with a standard DC load flow approximation. Each cascade of outages can be thought of as occurring once a day so that each day has one cascade. As expected in real power grids, most of the cascades consist of initial outages followed by no further outages, but quite often the initial outages propagate into further iterations of outages. An average daily peak load is chosen as the representative of the daily loading. It is necessary to provide some variation or noise in the input conditions to represent the varying conditions of the power grid so that a realistic variety of cascades can occur. This is done by making the pattern of loads for each day vary up and down randomly about the average daily peak load, and the magnitude of this load variation is controlled by the parameter γ .

In the fast time scale, each cascade of outages is produced iteratively. The iteration starts with a solved base case, which is then modified by independent random line outages with probability p_0 . Whenever a line is outaged, the generation is redispatched and the load is shed using standard linear programming optimization. The cost function is weighted to ensure that load shedding is avoided wherever possible. If any lines were overloaded during the optimization, then these lines are outaged with a fixed probability p_1 . If any line outages, then there is a further iteration of the process of redispatch and testing for outages. The iterations proceed until there are

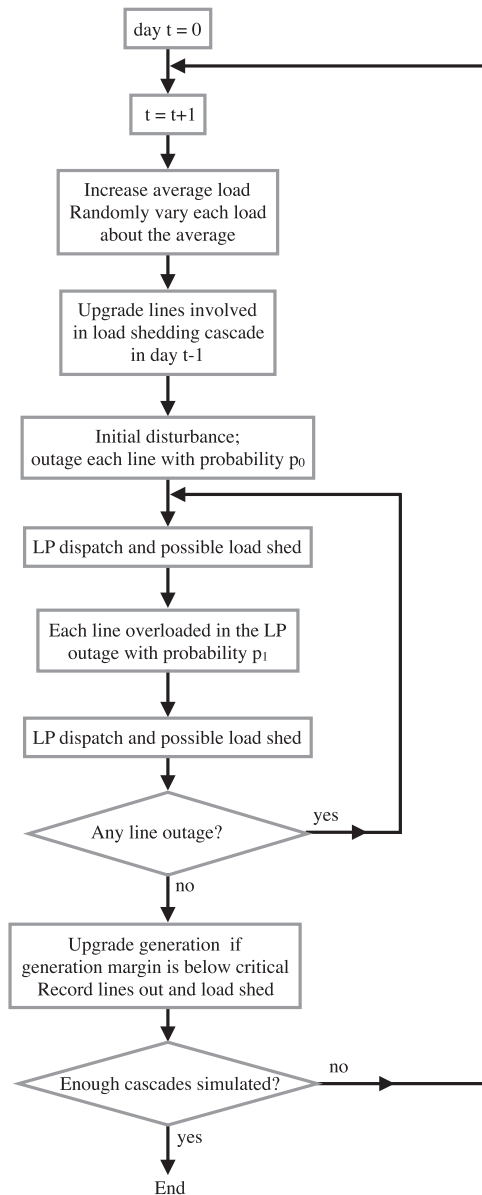


FIG. 1. OPA flow chart showing slow outer loop of grid evolution and fast inner loop of iterations of outages in each cascade.

no more outages. Then, the power lost in the blackout is the total load shed.

In the slow time scale, OPA models the complex dynamics of the transmission grid evolving in response to a slowly increasing power demand and, the increases in the system capacity are caused by the engineering responses to blackouts. The slow daily increase of the electricity demand is obtained by multiplying all loads by 1.00005, corresponding to the rate of increase of about 2% per year. If a blackout

occurs, then the lines involved in the blackout have their line flow limits increased slightly by multiplying by an upgrade parameter μ . That is, the parts of the system involved in the last blackout are upgraded. The grid topology remains fixed in the upgrade of the lines for model simplicity. To maintain a coordination between generation capacity and transmission capacity, the generation maximum power increases automatically when the capacity margin is below a given critical level $\Delta P/P$, which in the present case is taken to be 20%.

In this paper, we use an artificial network built according to the prescriptions of Ref. 16. The network has 1600 nodes and 2370 lines. This is large enough to be able to study the criticality issues. Networks with less than 400 nodes are not large enough for this purpose.

III. CRITICALITY METRIC λ_{gaga}

A self-organized critical system is by definition always close to a critical point, but the properties of this critical point may vary depending on different parameters that control the dynamics of the system. The OPA model with realistic grid parameters has the characteristics of a SOC system. However, when a wider range of parameters is considered, the complex dynamics of the cascading blackouts may change, move away from criticality, and other patterns of reliability emerge.

In Ref. 13, we introduced a metric λ_{gaga} that is a **generalized autonomous generational average (gaga)** to measure the proximity to criticality. To define λ_{gaga} , let us consider a time interval long enough to have many cascades during blackouts. Cascade length is the total number of iterations in a cascading process. Assume that j_M is the maximum number of iterations in the cascades during the period of time. Then for every $k < j_M$, we can calculate

$$\lambda_k(i) = \frac{O_k(i)}{O_k(i-1)}, \tag{1}$$

where $O_k(i)$ is the sum of the number of failures in iteration i for all cascades with length k or greater than k . Note the special case of $\lambda_0(i)$, which is the standard Harris estimator λ .¹⁴ Then, for $k > 2$, we define an average value of λ over the iterations, that is,

$$\langle \lambda \rangle_k = \frac{1}{k-2} \sum_{i=2}^{k-1} \lambda_k(i). \tag{2}$$

Then, λ_{gaga} is the averaged value over all values of the cut-off $k > 2$. It can be checked that $\langle \lambda \rangle_k$ converges quickly as k increases (see Ref. 13). This converged value can be interpreted as the averaged ratio of overloaded lines between consecutive iterations *particularized to long cascades*. To compare different states s , we define J_M to be the maximum value of j_M^s for different states. Then, $\lambda_{\text{gaga}}(s)$ is defined by

$$\lambda_{\text{gaga}}(s) = \frac{1}{J_M - 3} \sum_{k=3}^{j_M^s} \langle \lambda \rangle_k^s. \tag{3}$$

Because the value of $\langle \lambda \rangle_k$ saturates rapidly with growing k , $\lambda_{\text{gaga}}(s)$ can be roughly interpreted as the product of the saturated value and the cascade length. It thus weights both the length of the cascade and the ratio of overloaded lines between consecutive iterations for long cascades. This combination in a single parameter $\lambda_{\text{gaga}}(s)$ gives us a good measure of the proximity to the critical point, where the cascades are long and $\lambda_{\text{gaga}}(s)$ should peak. In particular, $\lambda_{\text{gaga}}(s)$ near one indicates criticality.

IV. HOW CRITICALITY AND PDFS DEPEND ON p_1

Let us consider the 1600 node network and study the dynamical evolution of this network for different values of p_1 . Figure 2 shows λ_{gaga} as a function of p_1 for the cascades of outages and overloads. Recall that in each iteration of OPA, the lines that outage are a subset of the lines that are overloaded and potentially outage, so that both the number of outages and the number of overloads produce a time series indicating the amount of cascading at each iteration. We can see that the values of λ_{gaga} are only close to one in a small interval of values of p_1 . When p_1 increases from zero to positive values, the system reaches a critical point around $p_1 = 0.024$. As p_1 continues to increase, finite size effects become important and, λ_{gaga} becomes at first stationary and then decreases. There are three regions: the first region is approaching criticality, the second is characterized by the competing effects of criticality and finite size, and the third is dominated by super-criticality and finite size effects. In this section, we analyze the properties of the three regions to see how the network complex dynamics have evolved.

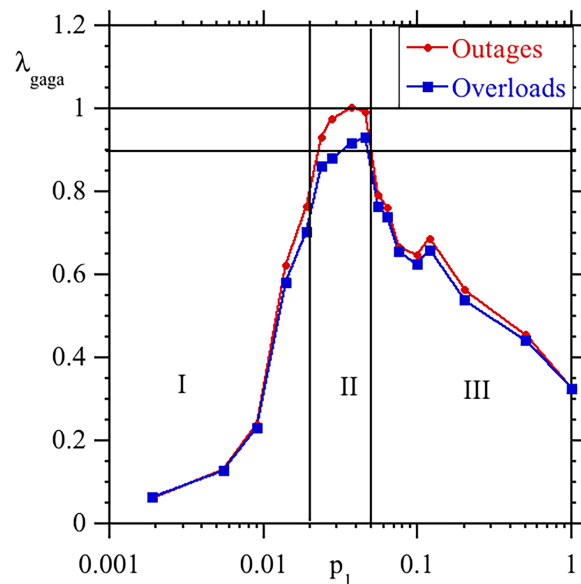


FIG. 2. λ_{gaga} as a function of p_1 for outages and overloads.

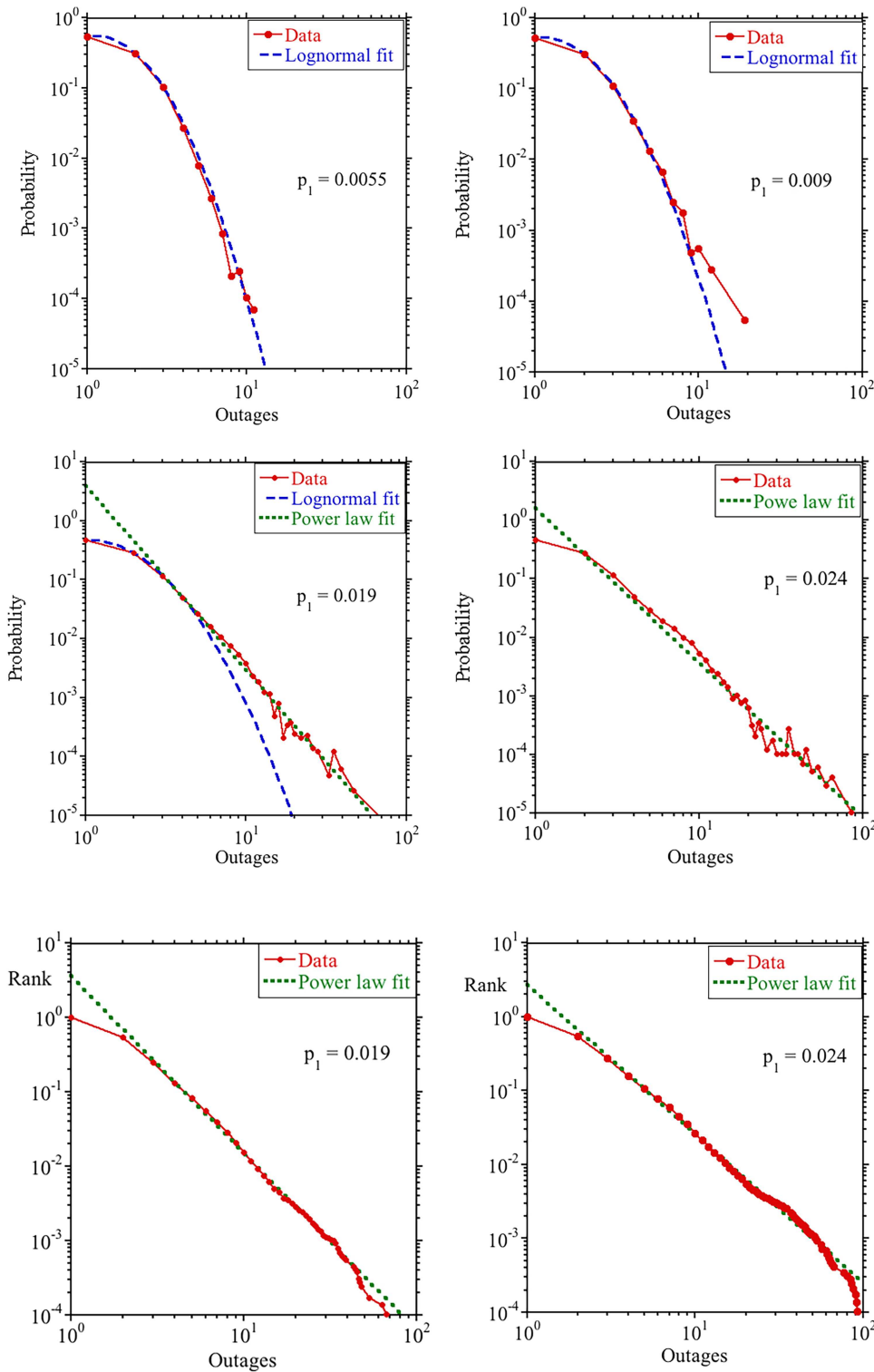


FIG. 3. PDF of line outages for four values of p_1 in Region I, with fits by lognormal (broken line) and the power law (dotted line) distributions.

FIG. 4. Rank function of line outages for two values of p_1 close to the critical region with power law fits.

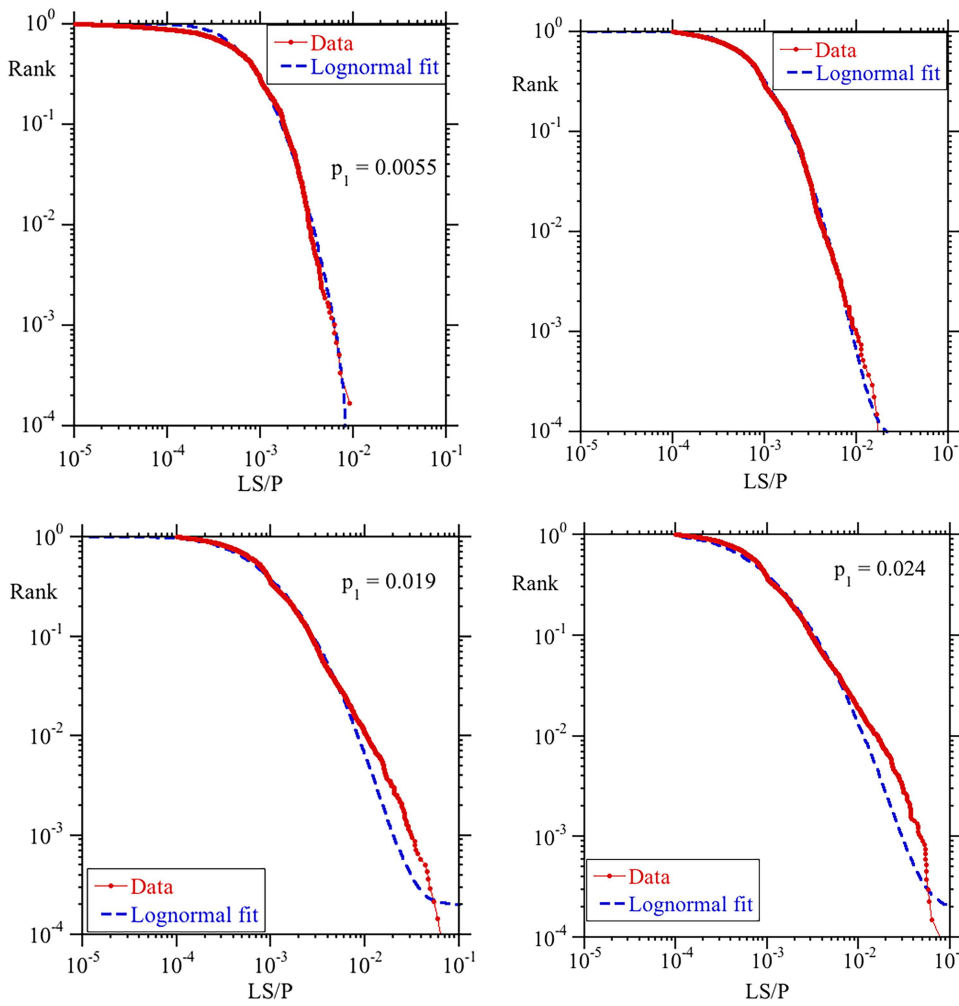


FIG. 5. Rank function of the normalized load shed with lognormal fits for four values of p_1 in Region I.

A. Region I: Approaching criticality

Let us consider the statistical data from the dynamical evolution of the network in Region I of Fig. 2, in which p_1 is in the range $[0, 0.024]$ and λ_{gaga} varies from 0 to 1. We first examine how the PDF of the number of outaged lines per blackout changes as p_1 increases in Region 1 as shown in Fig. 3. For very low values of p_1 , the PDF is well described by a lognormal distribution. As p_1 increases, a tail emerges in the PDF which has a power law character, and when p_1 is close to the critical point, almost the entire PDF becomes a power law. Of course, it is not easy to distinguish in some cases between a lognormal and a power law. This issue will be discussed in Sec. V. The situation bears a great similarity with the problem of drop fragmentation described in Ref. 6, which uses a simple model to describe the transition to criticality.

It is interesting to look in more detail at the two last cases in Fig. 3 that show a power law behavior of the tail. The power law dependence of the tail is even clearer in the rank function shown in Fig. 4. Furthermore, the exponents of the tail of the

PDF and rank function decrease as p_1 increases. Because of that, for the case of $p_1 = 0.0024$, it looks like finite size effects start to modify the end of the tail.

The change of the distribution from lognormal to power law can also be seen for the distribution of blackout size, measured by the power shed normalized by the total power demand. Figure 5 shows the rank function of the normalized load shed for the same values of p_1 used in Fig. 3. We observe the transition from one type of distribution to the other across those same values of p_1 .

B. Region II: Criticality

Region II is the criticality region in which p_1 is in the range $[0.024, 0.05]$. The PDF and rank functions for the blackout data in region II are very similar in the form to those in the upper part of region I (Figs. 4 and 5). However, the exponent of the power law for the rank function goes below 2 so that the tails of these functions become much less steep and as a

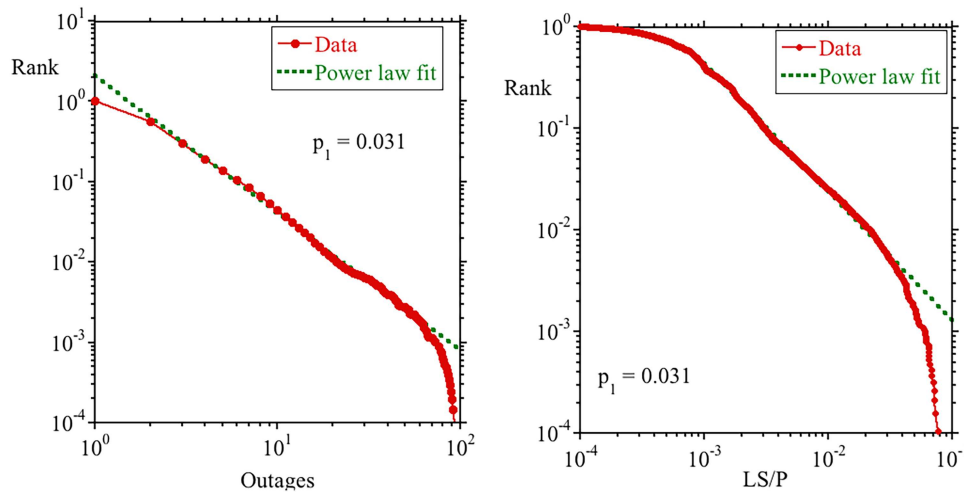


FIG. 6. Rank function of line outages and normalized load shed for $p_1 = 0.031$ in Region II with power law fits.

consequence, the finite size effects are more apparent. This can be seen in Fig. 6, where we have plotted for $p_1 = 0.031$ the rank function for both outages and normalized load shed.

C. Region III: Super-criticality

Region III is the region of low reliability of the lines, in which p_1 is in the range $[0.05, 1]$. In this region, lines outage easily and that changes the dynamics of the system. One of the consequences, as might be expected, is an increase of the frequency of the blackouts. Figure 7 shows the frequency of blackouts as a function of p_1 .

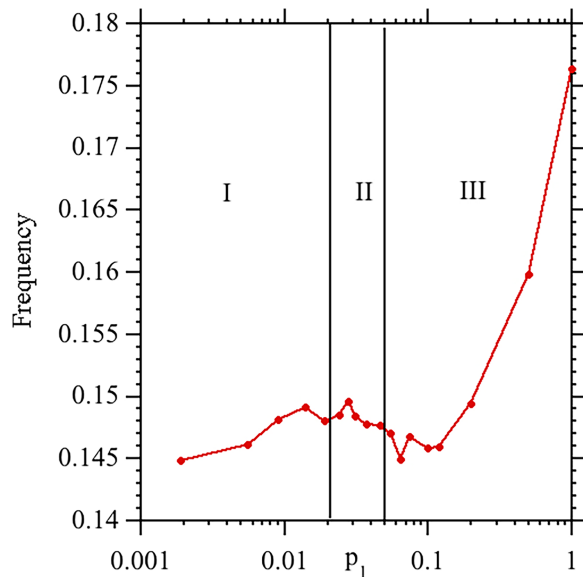


FIG. 7. Frequency of blackouts as a function of p_1 .

Another consequence of the low reliability of the lines is that the maximum length of the cascades decreases and as a consequence λ_{gaga} decreases as shown in Fig. 2. However, on average, the number of iterations of cascading increases. So the system is moving away from criticality as p_1 increases.

There are also changes in the PDF of the outages as p_1 increases. Figure 8 shows the PDF of outages for $p_1 = 0.12$. Figure 8 shows the PDF of the outages for all blackouts, for blackouts of only one iteration, and for the blackouts with more than one iteration. (Note that blackouts are defined as cascades that shed load.) Separating the PDF by the number of iterations shows two components. The PDF of the outages for blackouts with only one iteration peaks at one outage, but the data for this PDF are sparse and it is difficult to identify the form of this PDF. The PDF of the outages for blackouts with more than one iteration can be well described by a lognormal distribution, with the peak moving to a larger number of outages as p_1 increases.

For the real power grid, Region III is the least interesting region to consider. The electrical grids in developed countries do not operate in this low reliability region. The regimes to be considered in practice are Region II and the part of Region I close to Region II.

V. DETERMINING CREDIBLE POWER-LAW DISTRIBUTIONS

Section IV shows some rank functions of the blackout size that are compatible with a lognormal distribution or with a power-law distribution. To find which of these distributions is most credible, we use the criteria developed by Clauset *et al.*¹⁷

First, the minimum value of normalized load shed is determined by finding the minimal distance between the distribution of the power shed and its power law fit. The goodness of the fit test in Ref. 17 is done by generating samples of data based on the power law fit and by calculating the distance of these generated data from the power law fit. A measure p is the fraction of cases in which the distance of the generated

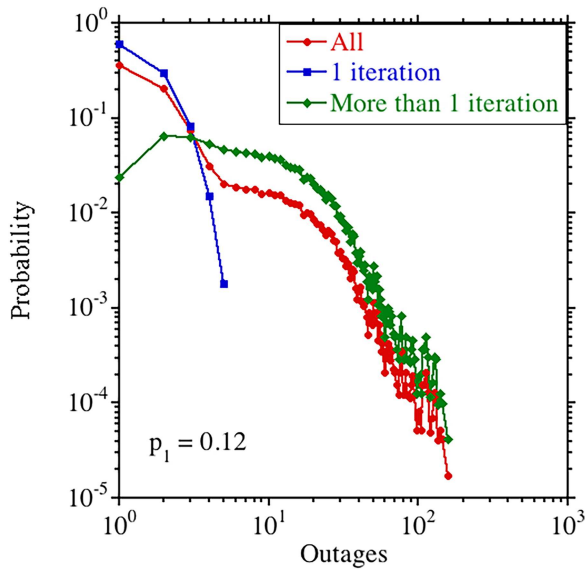


FIG. 8. Probability function of line outages for $p_1 = 0.12$ in Region III.

data to the fit is larger than the distance of the real data to the fit. A larger p indicates more confidence in the power law nature of the data, and we use $p > 0.1$ as a requirement for accepting the power law behavior. Another requirement that we impose is that the range of values of the power law be at least a decade. With these two requirements, we obtain the

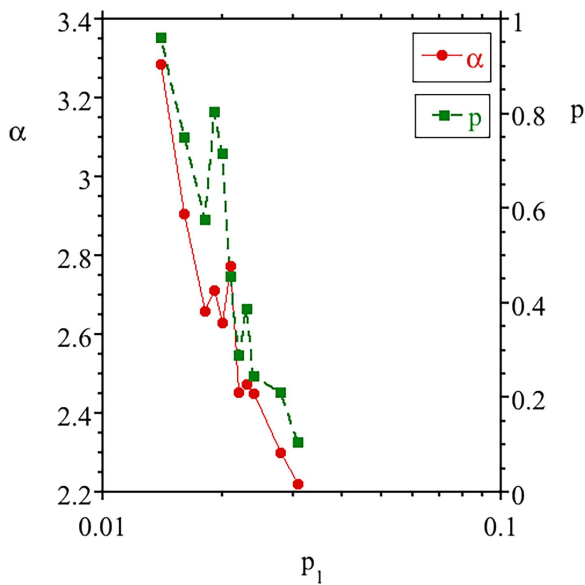


FIG. 9. Region of reliable power law behavior: α is the exponent of the tail of the PDF of blackout size and p the measure of goodness of the fit.

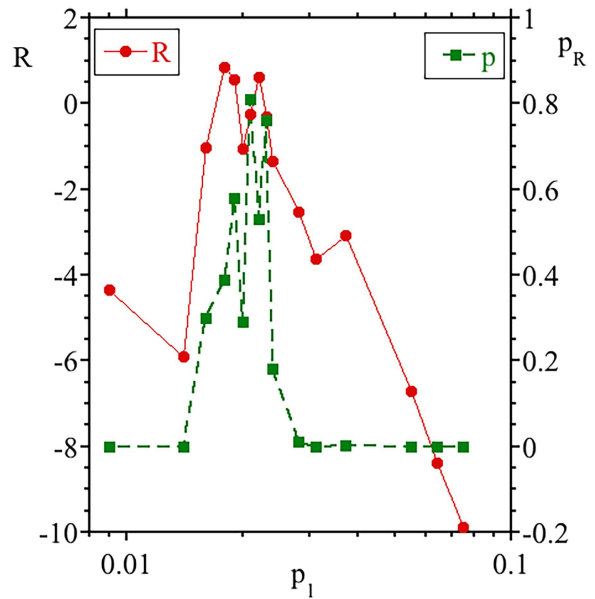


FIG. 10. R and p_R versus p_1 . $R > 0$ indicates power law is more likely and $R < 0$ indicates lognormal is more likely.

range of p_1 values with a credible power law shown in Fig. 9. The range of values of p_1 with a credible power law corresponds to the transition from region I to the critical region II in Fig. 2. As p_1 increases further in region II, the reliability of the power law fit decreases.

There is a further evaluation of the power law behavior which can be done by comparing the fits of the power law model with the lognormal model. As described in Refs. 17 and 18, the measure R can be introduced, which is the logarithm of the ratio of the likelihood for the two competing models. In our case, if R is positive, the power law has maximum likelihood, and otherwise the lognormal has maximum likelihood. The results as a function of p_1 are plotted in Fig. 10. We use the measure p_R that is related with the standard deviation of R to evaluate the significance of value of R (see Ref. 18). A smaller p_R indicates a less significant R . The criterion used in Ref. 17 for significance is $p_R < 0.1$. Figure 10 shows that the lognormal is the best model in the initial part of Region I and in Region III. In the range of p_1 shown in Fig. 9, consideration of R and p_R shows that the power law is possible. Overall, we can conclude that for p_1 in the approximate range $[0.018, 0.028]$, the power law is a possible fit for the distributions of the blackout measures.

VI. A SIMPLE MODEL OF THE LOGNORMAL BEHAVIOR AWAY FROM CRITICALITY

The results presented here bear a great similarity to the problem of drop fragmentation described in Ref. 15, where they use a simple model to describe a transition to criticality.

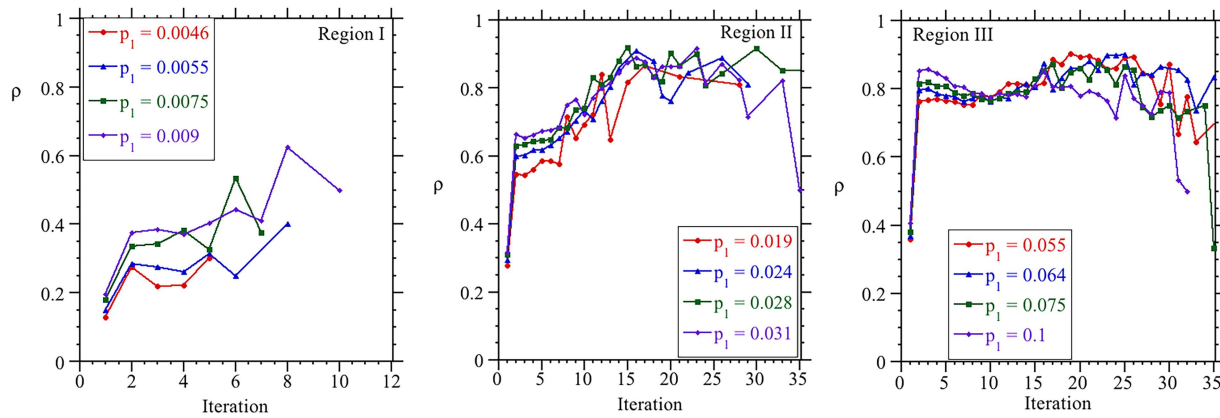


FIG. 11. The propagation function ρ as a function of the iteration number in the three regions defined in Fig. 2.

Here, in order to understand the basic characteristics of the critical point from the perspective of the cascade, we will use a quite similar approach.

From the perspective of analyzing the iterations of the cascading events, there is another way to characterize the proximity to criticality by examining the average propagation ρ as a function of the iteration number. The average propagation ρ is the probability of continuing the cascade at iteration k given that the cascade reached iteration k . Figure 11 shows the average propagation ρ as a function of the iteration number for different values of p_1 . We can see that in Regions I and III, ρ can be approximated as constant (note that the initial iteration contains initialization effects and that the final iterations have sparse data). On the other hand, in Region II, ρ at first increases with iteration number and then levels off. This is an indication that in regions I and III, the cascading process is practically randomly driven while region II is dominated by criticality behavior in which there are strong correlations.

We consider only Regions I and III, approximate the average propagation ρ as constant, and suppose that there is random variation about ρ as the cascade iterates. In particular, suppose that the propagation ρ_{jk} in iteration k of cascade j is

$$\rho_{jk} = \rho A_{jk}, \tag{4}$$

where A_{jk} are independent and identically distributed random variables of mean 1 and finite variance. The distribution of the number of iterations G_j in cascade j is given by

$$P[G_j \geq n] = \prod_{k=1}^{n-1} \rho_{jk} = \rho^{n-1} \prod_{k=1}^{n-1} A_{jk}, \tag{5}$$

$$P[G_j = n] = (1 - \rho A_{jn}) \prod_{k=1}^{n-1} (\rho A_{jk}). \tag{6}$$

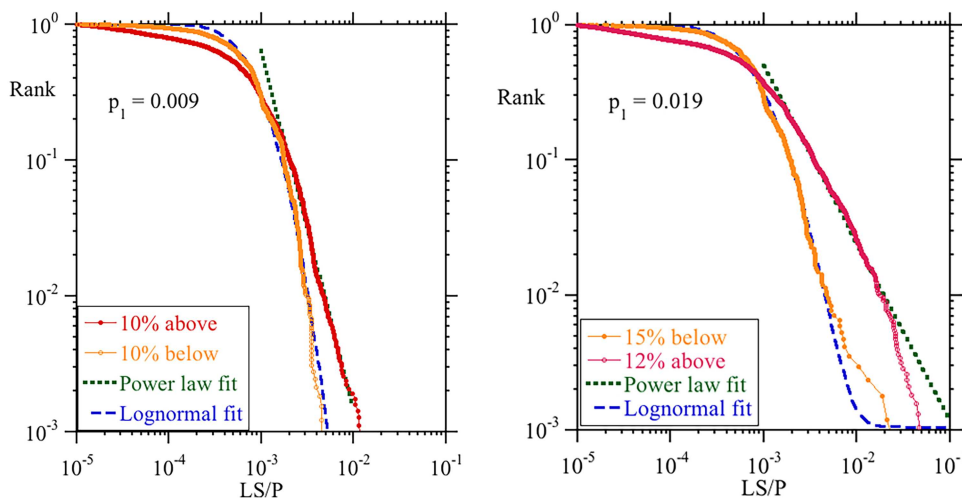


FIG. 12. Rank function of the normalized power shed for states with demand above and below the averaged demand and two values of p_1 in Region I with fits by a lognormal (broken line) and power law (dotted line) distributions.

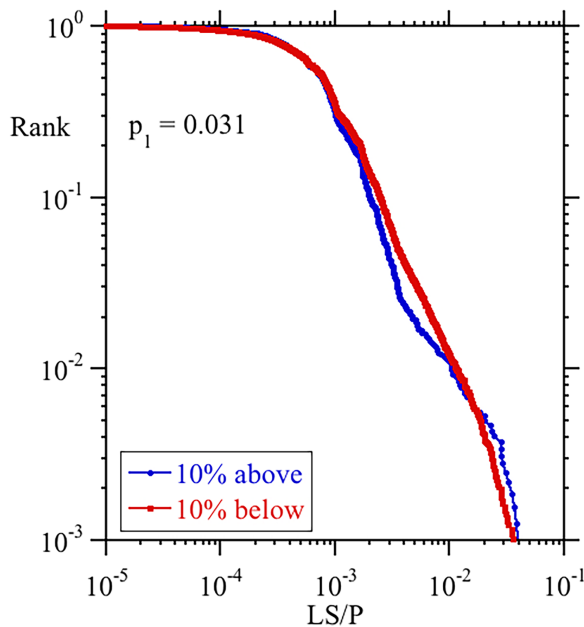


FIG. 13. Rank function of the normalized power shed for states with demand above and below the average demand with $p_1 = 0.031$ in Region II.

So the process being multiplicative and the central limit theorem indicate a lognormal form of the distribution of G for large enough n .

If w is the average number of line outages per iteration, the expected total number of outages for n iterations is

$$ET = \sum_{k=1}^n wP[G \geq n] = w(1 + \rho + \rho^2 + \dots + \rho^{n-1}) = w \frac{\rho^n - 1}{\rho - 1}, \tag{7}$$

so if $\rho = 1$, there is a critical point and the sum diverges.

In light of what we have described in Sec. III and in Fig. 2, the multiplicative model is consistent with the dynamics in Regions I and III of Fig. 1 because the propagation probability ρ is practically constant in Regions I and III. However, the multiplicative model does not describe the dynamics in the critical Region II.

VII. STATES WITHIN A SINGLE DYNAMICAL EVOLUTION WITH DIFFERENT LEVELS OF CRITICALITY

For a fixed set of parameters, the dynamical evolution of OPA leads to multiple states with different levels of power demand and different potential blackout properties. Not all these states can lead to the same type of blackout nor to the same cascade of events. Even if the system is in Region II, not all events have the properties of a critical event, and we can analyze now sets of these states from the perspective of criticality.

We can use the power demand to classify these states. The average power demand ($\langle P_d(t) \rangle$) is increasing with time and we can normalize the difference between the daily power demand $P_d(t)$ and the average power demand ($\langle P_d(t) \rangle$) to obtain

$$\Delta P = \frac{P_d(t) - \langle P_d(t) \rangle}{\langle P_d(t) \rangle}. \tag{8}$$

The value of ΔP allows us to classify states with power demand more than a fraction above the mean power demand or more than fraction below the mean power demand. When we look at the rank function of the normalized load shed, we can see a clear difference between the states with demands above and below the mean. Figure 12 shows two examples of cases in Region 1.

As mentioned before, it is not clear when a PDF or a rank function can be fitted by a lognormal or a power law PDF. However, if we assume a power law, it is clear that the exponent for the rank of the states above the mean is smaller than for those below the mean. For the case with $p_1 = 0.019$ in Region I, the exponent for the cases below the mean is less than 2, which is an exponent corresponding to Region II, the critical region. So even if the overall case is subcritical, it contains many states that are critical.

When the system is in the critical region, Region II, there is no clear distinction between the states above the average demand and below as can be seen in Fig. 13 for $p_1 = 0.031$.

VIII. CONCLUSIONS

In this paper, we have discussed the level of criticality of the solutions of the OPA model depending on the reliability of the network, as measured by the parameter p_1 that describes the line reliability by controlling the overloaded line outage probability. We have shown that for low values of p_1 (high reliability lines), distributions of load shed and outages are essentially a lognormal distribution. As the system lines become more unreliable, p_1 increases, and we reach a critical region in which the distributions show a power tail. When the system lines become very unreliable, the system goes supercritical and the distributions became lognormal again.

The calculations have been done for a model network. The observed data in the power grid⁴ and the modeling with OPA of WECC networks and other simulations^{4,5,11,19} show that the real power networks are generally in the transition region from subcritical to critical.

ACKNOWLEDGMENTS

The simulation runs have been carried out on Uranus, a supercomputer cluster located at Universidad Carlos III de Madrid and funded jointly by EU-FEDER funds and by the Spanish Government via the National Project Nos. UNC313-4E-2361, ENE2009-12213-C03-03, ENE2012-33219, ENE2012-31753, and ENE2015-68265-P. J.M.R.-B. acknowledges useful interactions with members of the research network “Avalanchas en biofísica, geofísica, materiales y plasmas,”

funded by the Spanish Government Project No. MAT2015-69777-REDT. I.D. acknowledges funding from the National Science Foundation (NSF) (Grant Nos. 1609080 and 1735354). We thank Zhifang Wang for generously sharing code for constructing the artificial network.

REFERENCES

- ¹B. A. Carreras, D. E. Newman, I. Dobson, and A. B. Poole, "Evidence for self organized criticality in a time series of electric power system blackouts," *IEEE Trans. Circuits Syst. Part I* **51**(9), 1733–1740 (2004).
- ²P. Hines, J. Apt, and S. Talukdar, "Large blackouts in North America: Historical trends and policy implications," *Energy Policy* **37**, 5249–5259 (2009).
- ³B. A. Carreras, V. E. Lynch, I. Dobson, and D. E. Newman, "Complex dynamics of blackouts in power transmission systems," *Chaos* **14**(3), 643–652 (2004).
- ⁴J. Chen, J. S. Thorp, and I. Dobson, "Cascading dynamics and mitigation assessment in power system disturbances via a hidden failure model," *Int. J. Electr. Power Energy Syst.* **27**(4), 318–326 (2005).
- ⁵D. P. Nedic, I. Dobson, D. S. Kirschen, B. A. Carreras, and V. E. Lynch, "Criticality in a cascading failure blackout model," *Int. J. Electr. Power Energy Syst.* **28**, 627–633 (2006).
- ⁶D. E. Newman, B. A. Carreras, V. E. Lynch, and I. Dobson, "Exploring complex systems aspects of blackout risk and mitigation," *IEEE Trans. Reliab.* **60**(1), 134–143 (2011).
- ⁷D. E. Newman, B. A. Carreras, N. S. Degala, and I. Dobson, "Risk metrics for dynamic complex infrastructure systems such as the power transmission grid," in *Forty-Fifth Hawaii International Conference on System Sciences* (IEEE, Maui, Hawaii, 2012).
- ⁸I. Dobson, B. A. Carreras, V. E. Lynch, and D. E. Newman, "Complex systems analysis of series of blackouts: Cascading failure, critical points, and self-organization," *Chaos* **17**, 026103 (2007).
- ⁹S. Mei, X. Zhang, and M. Cao, *Power Grid Complexity* (Tsinghua University Press, Springer, Beijing, 2011).
- ¹⁰P. Bak, C. Tang, and K. Wiesenfeld, "Self-organized criticality: An explanation of $1/f$ noise," *Phys. Rev. Lett.* **59**, 381 (1987).
- ¹¹B. A. Carreras, D. E. Newman, I. Dobson, and N. S. Degala, "Validating OPA with WECC data," in *46th Hawaii International Conference on System Science* (IEEE, 2013).
- ¹²B. A. Carreras, J. M. Reynolds-Barredo, I. Dobson, and D. E. Newman, "Validating the OPA cascading blackout model on a 19402 bus transmission network with both mesh and tree structures," in *52nd Hawaii International Conference on System Science* (IEEE, 2019).
- ¹³B. A. Carreras, D. E. Newman, and I. Dobson, "Lambda-Gaga: Toward a new metric for the complex system state of the electrical grid," in *48th Hawaii International Conference on System Science* (IEEE, 2015).
- ¹⁴T. E. Harris, *Theory of Branching Processes* (Dover Pubns, Dover, NY, 1989), ISBN 10: 0486659526, ISBN 13: 9780486659527.
- ¹⁵O. Sotolongo-Costa, Y. Moreno-Vega, J. J. Lloveras-Gonzalez, and J. C. Antoranz, "Criticality and droplet fragmentation," *Phys. Rev. Lett.* **76**, 42 (1996).
- ¹⁶Z. Wang, A. Scaglione, and R. J. Thomas, "Generating statistically correct random topologies for testing smart grid communication and control networks," *IEEE Trans. Smart Grid* **1**(1), 28–39 (2010).
- ¹⁷A. Clauset, C. R. Shalizi, and M. E. J. Newman, "Power-law distributions in empirical data," *SIAM Rev.* **51**(4), 661–703 (2009).
- ¹⁸Q. H. Vuong, "Likelihood ratio tests for model selection and non-nested hypotheses," *Econometrica* **57**(2), 307–333 (1989).
- ¹⁹B. A. Carreras, D. E. Newman, and I. Dobson, "North American blackout time series statistics and implications for blackout risk," *IEEE Trans. Power Syst.* **31**(6), 4406–4414 (2016).